Research Article | Vol. 28, No. 8 / 13 April 2020 / Optics Express 11406
Optics EXPRESS

Mimicking an expanding universe by optical interference in a helicoid waveguide

GUO-HUA LIANG,[1] RONG G. CAI,[2] YIN-ZHE MA,[3,4] RUN-QIU HE,[1] SHINING ZHU,[1] AND HUI LIU[1,*]

[1]National Laboratory of Solid State Microstructures and School of Physics, Collaborative Innovation Center of Advanced Microstructures, Nanjing University, Nanjing 210093 Jiangsu, China
[2]CAS Key Laboratory of Theoretical Physics, Institute of Theoretical Physics, Chinese Academy of Sciences, Beijing 100190, China
[3]School of Chemistry and Physics, University of KwaZulu-Natal, Westville Campus, Private Bag X54001, Durban 4000, South Africa
[4]NAOC–UKZN Computational Astrophysics Centre (NUCAC), University of KwaZulu-Natal, Durban 4000, South Africa
*liuhui@nju.edu.cn

Abstract: According to modern cosmology, expansion of the universe is due to the metric changing of spacetime itself. Here, we propose to mimic an expanding universe by utilizing optical interference and helicoid waveguides. The evolution of interference pattern in the helicoid waveguide is investigated theoretically and experimentally. For precise measurements, we design an air helicoid waveguide which allows us to investigate the wave front of laser beams from the waveguide. Redshift of a Gaussian wave packet in the expanding universe is demonstrated with high precision, showing that the helicoid waveguide acts as a parabolic gradient index lens exactly. The proposed waveguide structure can be used as an efficient waveguide adapter.

1. Introduction

Since 1920s, the expansion of the universe has been proposed and observed by a few pioneer astronomers (e.g. George Lemaitre in 1927 and Edwin Hubble in 1929) by measuring the receding velocities of nearby galaxies [1]. In the recent 20 years, astronomical surveys in multi-wavelength regime have progressed very fast and measured the cosmic expansion rate very accurately through the observations of cosmic microwave background radiation [2], the baryon acoustic oscillation from galaxy spectroscopic survey [3] and the luminosity distance of Type-Ia supernovae data [4]. These data from large-scale structure of the Universe have provided abundant information, but also challenged our understanding about the nature of the expansion of the spacetime. So far, theoretical models vary about the reason of expansion. More information is needed in the development of the underlying theory. Nevertheless, in recent years, more and more [5–13] types of general relativity analogues have been found in condensed matter and optical systems. To demonstrate theoretical models and improve our understanding, it is very helpful to build experimental analogue systems in the laboratory and exhibit the simulated phenomena of the expanding spacetime.

Analogue gravity has been studied in various table experimental systems. In 1981, W.G. Unruh theoretically proposed the hydrodynamical analog of an event horizon [14], which is based on the mathematical similarity between the motion of sound waves in a convergent fluid flow and the behavior of a scalar field in a classical gravitational background. Since then, various realizations have been performed for the analog of Hawking radiation, such as surface waves on moving water [15], Bose-Einstein condensates [5–8], Fermi-degenerate liquids [9], ion rings [10], polariton fluids [11] and nonlinear optical fiber horizon [12,13].

#392564 https://doi.org/10.1364/OE.392564
Journal © 2020 Received 11 Mar 2020; revised 26 Mar 2020; accepted 27 Mar 2020; published 1 Apr 2020

Optics EXPRESS

Besides, because of the equivalence between the Maxwell equations in curved space-time and those in the corresponding complex inhomogeneous medium [16], transformation optics [17–19] was introduced to control light artificially [20–22] and utilized to simulate the analog effects of general relativity [23], such as black holes [24–28] and wormholes [29–31], Rindler spacetime and cosmic strings with metasurfaces [32,33], and quantum simulation in curved space with photonic lattices [34,35]. Recently, people have tried to mimic gravity by fabricating curved two-dimensional (2D) waveguides [36–39]. Compared with the inhomogeneous materials, curved waveguides are easier to be realized and manipulated. In these waveguides, the scalar property of light is governed by the d'Alembertian equation in the corresponding 2D curved space [40]. By making use of this fact, diffraction [36], correlation length [37], group and phase velocities [38] of beams have been studied in various structures with positive or negative intrinsic curvature.

Cosmic expansion is also of high interest for modeling in various systems. The feasibilities of different modeling schemes have been discussed by early theoretical works [41–48]. In recent years, a few experiments have been performed [49,50]. For instance, supersonically expanding and ring-shaped atomic Bose-Einstein condensate have been used to study the dynamics of an expanding universe [49]. In optics, plasmonic hyperbolic materials have been adopted to emulate a big-bang-like event [50]. As we know, the expansion rate, shown by the scale factor in the Friedmann-Robertson-Walker (FRW) metric, is a varying function with the evolution of the universe, and is also the key term to distinguish different universe models. Therefore, precise controlling of the expanding acceleration of the analog universe is necessary. As far as we know, there is still no report to investigate the expansion of the universe through controlling the expanding acceleration in an experiment.

In this work, we propose helicoid waveguides to mimic the expanding universe in optical experiments. We devise an air helicoid waveguide which is obtained with an air layer sandwiched by two metal helicoid surfaces, which efficiently avoids interface scattering when the laser beams enter and leave the waveguide, allowing us to measure the output laser patterns with high accuracy. Since the metal surfaces are controllable by 3D print technique, the expanding rate of the analog universe can also be defined exactly. In the following, we will describe the theory framework, the experimental platform and the experimental results.

2. Model and theory

In standard cosmology, FRW metric describes a spatially homogeneous and isotropic universe, which can be written as

$$\mathrm{d}s^2 = -\mathrm{d}t^2 + a^2(t)\left[\frac{\mathrm{d}r^2}{1-Kr^2} + r^2\mathrm{d}\theta^2 + r^2\sin^2\theta\mathrm{d}\phi^2\right], \tag{1}$$

where t is the cosmic time, r, θ, φ are comoving coordinates, $a(t)$ is the scale factor and K is the spatial curvature parameter, with $K = 0$ for the Euclidean space, $K>0$ for the spherical case and $K<0$ for the hyperbolic case. Here we have set the speed of light $c = 1$. In this $3+1$ dimensional metric, the comoving radial distance is defined as $\chi = \int_0^r dx/\sqrt{1-Kx^2}$, which is time independent. In contrast, the proper radial distance .. varies as a function of time because of the expansion of the universe. It is clear that the comoving distance is equal to the proper distance at the present time t_0 by taking $a(t_0) = 1$. Hubble parameter is defined as $H = \dot{a}/a$, where the overdot denotes derivative with respect to t.

In our work, we consider the $1+1$ dimensional FRW metric

$$\mathrm{d}s^2 = -\mathrm{d}t^2 + a^2(t)\mathrm{d}\chi^2. \tag{2}$$

Experimentally, we design a helicoid waveguide to represent the space-time described by the metric [Eq. (2)], which is shown in Fig. 1(a). In Euclidean space, this helicoid surface can be

Optics EXPRESS

parameterized as $X = T\cos\omega\chi'$, $Y = T\sin\omega\chi'$, $Z = \chi'$, where χ', T are spatial coordinates, and ω is a constant parameter. Based on the quantum-optical analogies [51], T can be used to represent the cosmic time t, and χ' is still a spatial coordinate. We can see that the surface is formed by the time arrow T rotating around χ' axis with constant angular speed ω while moving along this axis. Corresponding to the FRW metric, we define the present time as T_0, which means $a(T_0) = 1$, and $T<T_0$ represents the past. The curvilinear coordinate axis χ is the blue line shown in Fig. 1(a). In this figure, points A and A' have the same comoving coordinate .. and different time coordinate T, so do B and B'. Therefore, the comoving distance between A' and B' is the same with A and B, which is $|\chi_B - \chi_A|$, while the proper distance $d_p = a(T)\chi$ between A′ and B′ is $|\chi'_{B'} - \chi'_{A'}|$.

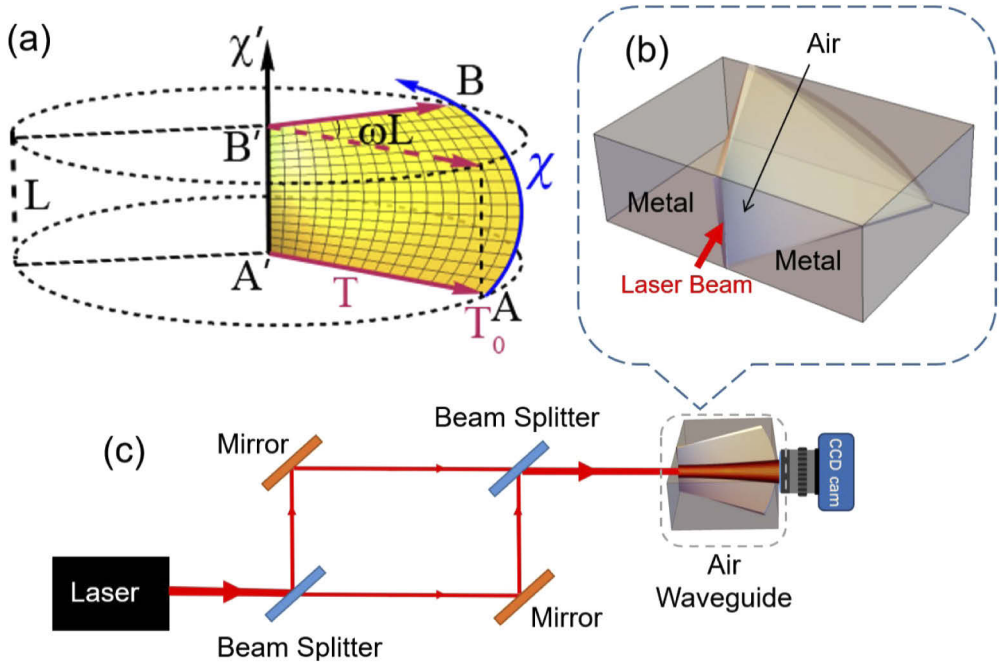

Fig. 1. (a) A helicoid surface with its structure parameters. (b) An air helicoid waveguide sandwiched by two metals. (c) Experiment setup of two-beam interference.

First, we give a brief description on the propagation of a light beam inside the helicoid waveguide theoretically. If we consider only the scalar property of light, the light field satisfies the Helmholtz equation [40]

$$\left[k^2 + \partial_T^2 + H\partial_T + \frac{1}{a^2(T)}\partial_\chi^2\right] E(\chi, T) = 0\,, \tag{3}$$

where $k = 2\pi/\lambda$ with λ the wavelength, and $E(\chi, T)$ is the electric component of the light field. We assume the input laser beam is monochromatic and paraxial along the T direction, and make the ansatz $E(\chi, T) = \phi(\chi, T)e^{ikT}/\sqrt{a(T)}$, then Eq. (3) can be approximately reduced to the paraxial equation

$$\left(2ik\partial_T + \frac{1}{a^2(T)}\partial_\chi^2 + V_{\text{eff}}\right)\phi(\chi, T) = 0\,, \tag{4}$$

where $\phi(\chi, T)$ is the rescaled field amplitude and $V_{\text{eff}} = (\dot{a}^2 - 2a\ddot{a})/4a^2$. We can find this equation is similar to a Schrödinger equation in the 1 + 1 dimensional FRW metric. By defining a new

Optics EXPRESS

wavefunction $u = \phi \exp \int -\frac{i}{2k} V_{\text{eff}}(T')dT'$ and performing a coordinate transformation

$$\tilde{T} = \int_0^T 1/a^2(x)dx, \tag{5}$$

Equation (4) can be further reduced to a flat Schrödinger equation, which gives us the corresponding Green's function easily.

Considering all the manipulation above, we obtain the final Green's function

$$G(\chi, T; \bar{\chi}, 0) = \sqrt{\frac{k}{2\pi i a \tilde{T}}} e^{i\frac{k}{2\tilde{T}}(\chi-\bar{\chi})^2} e^{\frac{i}{2k}\int_0^T V_{\text{eff}}(T')dT'} e^{ikT} . \tag{6}$$

It is worth noting that the second and third exponential factor in Eq. (6) is independent of the transverse coordinate, therefore when we calculate the transverse distribution of the light at a certain propagation distance, they cancel out. Making use of the Green's function, we can track the evolution of the beam in the surface and get the amplitude at any time

$$E(\chi, T) = \int \mathrm{d}\overline{\chi}\, G(\chi, T; \bar{\chi}, 0)\, E(\bar{\chi}, 0) . \tag{7}$$

Based on Eqs. (6) and (7), by calculating the intensity $|E(\chi, T)|^2$ of a Gaussian beam, we can immediately find how the beam width varies in the helicoid waveguide. We assume the initial profile of the Gaussian beam at the input is $E(\chi', 0) = E_0 e^{-\frac{\chi'^2}{2w_0}}$, where the initial width is w_0 and E_0 is a constant. Substituting this initial profile into Eq. (7), and perform integration by using the formula for the integral of Gaussian function $\int_{-\infty}^{\infty} e^{-ax^2+bx+c}dx = \sqrt{\pi/a}\, e^{\frac{b^2}{4a}+c}$, we eventually arrive at $|E(\chi, T)|^2 = E_0^2 \frac{w_0}{w(T)} e^{-\frac{\chi^2}{w^2(T)}}$, where the beam width is

$$w(T) = w_0\sqrt{1+\omega^2T^2}\sqrt{1+\frac{\arctan^2\omega T}{\omega^2k^2w_0^4}}. \tag{8}$$

In the calculating process, we use $\tilde{T} = \frac{\arctan \omega T}{a^2(0)\omega}$ and make the substitution $\chi = \sqrt{1+\omega^2T^2}\chi'$. In Eq. (8), the term $\frac{\arctan^2\omega T}{\omega^2k^2w_0^4}$ depends on the geometric parameter ω and the propagation constant k. If we let $\omega \to 0$, the width $w(T) = w_0\sqrt{1+T^2/k^2w_0^4}$, which exactly gives the diffraction of Gaussian beam in flat space. In addition, the geometric parameter ω determines the curvature of the helicoid. Hence this term reflects the combined effect of diffraction and curvature of the waveguide on the beam. Neglecting this term, the beam expanding as the space of the analog universe.

Theoretically we assume the Gaussian laser beams are totally coherent, in the air waveguide, the amplitude of two coherent beams at $T = 0$ can be written as

$$E_{1,2}(\chi', 0) = E_0 e^{-\frac{\chi'^2}{2w_0^2}} e^{ik_{1,2}\chi'}, \tag{9}$$

where $k_1, k_2 \ll k$ denote tiny momentum in the χ' direction for the two beams, respectively.

Performing the same calculation procedure for the Gaussian beam, we can obtain the evolution of both laser beams in the waveguide. If the two beams get close enough, interference happens

Optics EXPRESS

and the intensity distribution would be

$$I = |E_1|^2 + |E_2|^2 + E_1^* E_2 + E_2^* E_1. \tag{10}$$

By neglecting a phase term which is χ independent and very closed to one, we find the intensity could be expressed in the form

$$I(\chi, T) = I_0 e^{-\frac{\chi^2}{(1+\omega^2 T^2)\left[w^2+\left(\frac{\arctan \omega T}{\omega k w}\right)^2\right]}} \left(1 - \cos\left[\frac{(k_1 - k_2)\chi}{\sqrt{1+\omega^2 T^2}\left(1+\left(\frac{\arctan \omega T}{\omega k w^2}\right)^2\right)}\right]\right). \tag{11}$$

Note that the coordinates have the relation $\chi = \chi'/a(0)$. Again, in Eq. (11), we find the effect from diffraction and curvature on the period of the interference fringes. In our experiment, $k \sim 10^4 \text{mm}^{-1}$ and $w = 0.45$mm, which means $\omega k w^2 \gg 1$, implying that this effect can be neglected and the period of the fringes of the output spot at $T = T_0$ is $\Delta\chi = 2\pi\sqrt{1+\omega^2 T_0^2}/|k_1 - k_2|$. Therefore, the laser beam spread along the camber coordinate net showed in Fig. 1(a). The interference pattern at the output spot should be distributed along the curved χ coordinate axis direction. However, since the output spot is small enough compared with the curvature radius of χ axis, the wave front of the output spot is nearly a plane. Therefore, the measurement by a planar CCD camera is accurate. It should be mentioned that if we adopt the laser beam thin enough and the CCD camera with higher resolution, the effect from diffraction and curvature may have measurable influence.

3. Experiment and discussion

In the following, we experimentally simulate the redshift of a Gaussian wave packet in the expanding universe through optical interference of two laser beams in helicoid waveguide. Cosmological redshift is a very important phenomenon in modern cosmology [52]. The wavelengths of photons from different distances propagating through the expanding space are stretched to different extents, which enable us to acquire the information of the universe expansion. In this experiment, the FRW space-time is mimicked by a helicoid air waveguide sandwiched between two metals as shown in Fig. 1(b). The advantage of the air waveguide compared with polymer waveguide is to avoid the interface scattering, enabling the laser beam enter and leave the air waveguides with small scattering loss and high-quality beam spot. This advantage allows us to investigate the wave front of the propagating beam in curved space directly, which has not been done in previously relevant works. We set the structure parameters as $T_0 = 20$mm and $\omega = \pi/4$ rad/cm in this design. These geometric parameters are alterable by using 3D print technique.

In the experiment, we input two laser beams into the waveguide and take image of input and output beam spot (see Fig. 1(c)). In the experiment, the incident position is at $\chi' = L/2$. In fact, the incident position does not affect the result since the analog space is homogeneous everywhere. The laser beam should be orthogonal to the χ' axis and parallel to the T axis at the input position. The propagation of the coherent beams is well described by paraxial wave optics. The two beams interfere with each other before they enter the air waveguide. Then the intensity function at $T = 0$ is given by $I(x) = 2I_0 \exp(-x^2/w_0^2)\cos^2(\Delta k x/2) = |\psi(x)|^2$, where x is the transverse coordinate, $\Delta k = |k_1 - k_2|$ and I_0 is a constant parameter. Here, we find this intensity function allows us to define a wave packet ψ and its wave number $\nu = \Delta k/2$, then the fringe period Δx is taken as the wavelength Λ. From the cosmological standpoint, redshift caused by the universe expansion leads to the relation $\Lambda(t_2) = \Lambda(t_2)a(t_1)/a(t_2)$, which indicates $\Delta x(T_1) = \Delta x(T_2)a(T_1)/a(T_2)$ in the experiment. Hence by measuring the time dependence of the intervals $\Delta x(T)$, we can emulate the

Optics EXPRESS

redshift of the wave packet during the expansion of the universe. The input and output beam spots are given in Figs. 2(d) and 2(e). We numerically calculate the evolution of the interference pattern inside the waveguide shown in Fig. 2(c). Figures 2(a) and 2(b) show the numerical results of the input and output beam spots, which are in good agreement with the corresponding experimental images in Figs. 2(d) and 2(e). It is evident that the interval Δx becomes larger from the input spot to the output spot, which gives a good simulation of the redshift of a Gaussian wave packet in the expanding universe.

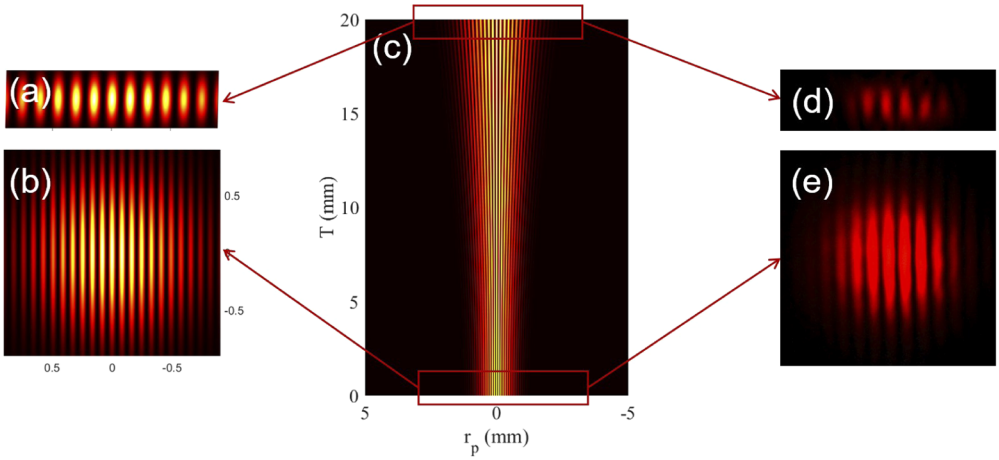

Fig. 2. (a) The calculated output (a) and input laser spot (b). (c) Numerical calculation results of the interference pattern of two coherent beams during propagation. The measured output (d) and input (e) laser spot.

In Fig. 3(a), we present the interference fringes of the input (blue dashed line) and output spots (red solid line) simultaneously. The periods of two spot patterns, $\Delta x(0)$ and $\Delta x(T_0)$, can be determined through measuring the distance between two neighbor ditches in the periodic fringes. Theoretically, from the geometric parameters of the helicoid waveguide, the scale factor at $T = 0$ is $a_{\text{th}}(0) = 1/\sqrt{1+\omega^2 T_0^2} = 1/1.8621$. In Fig. 3(b), the positions of the ditches for the input and output spot show a good linear function dependence, indicating the expanding of the pattern in the experiment is spatially homogeneous. From the linear function in the figure, we can obtain the experimental value of the scale factor at the input location (the past) as $a_{\text{exp}}(0) = 1/1.8663$, in accordance with the theoretical value $a_{\text{th}}(0)$. Then the redshift parameter [52] can be obtained as $z(0) = 1/a(0) - 1 = 0.8663$. Figure 3(c) provides the redshift $z(T)$ obtained from the numerical calculation (red circle) and experimental data (purple cross), respectively. Here, the numerical results of $z(T)$ are obtained from the results in Fig. 2(c). The experimental value is in good agreement with the theory and numerical value at the output spot, demonstrating the cosmic redshift quite well.

The experimental results above show that the interference pattern of the laser beams can be used like a ruler to measure the expanding of the analog universe. In fact, the homogeneous expansion of the beam in our helicoid waveguide is an experimental realization of a parabolic gradient-index lens [48]. If we replace the interference pattern by the source of digital coding information at the input, the waveguide exactly plays a role of a lossless adapter or a signal spreading device, connecting waveguides with different sizes efficiently, as ideally this structure maintains the shape of the original wave packet no matter what shape it is.

Optics EXPRESS

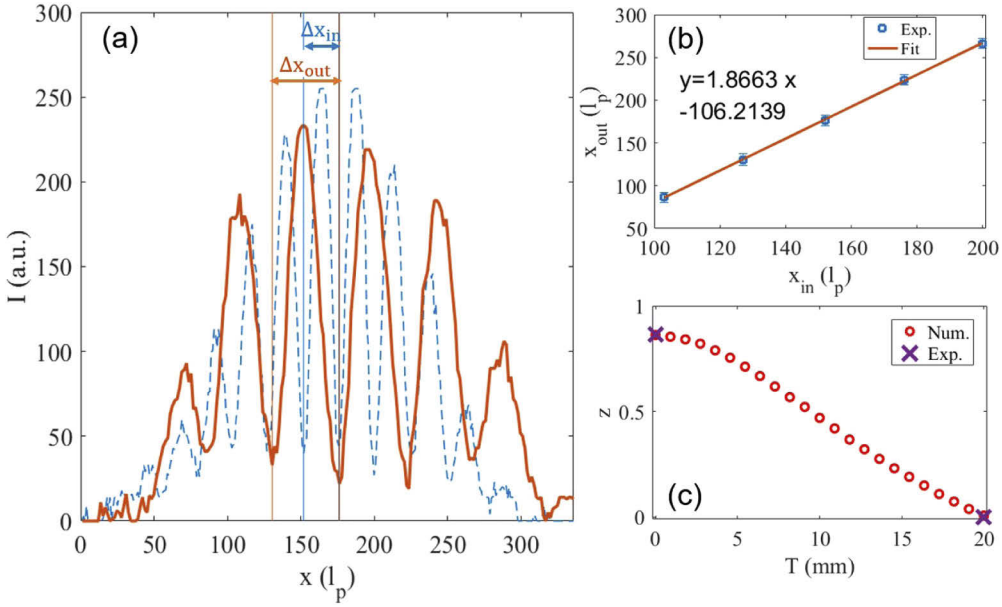

Fig. 3. (a) The measured intensity profile of input (blue line) and output (red line) laser beam spots; The pixel size of the CCD camera $l_p = 3.75\mu m$. (b) The linear dependence between period of input spot and out spot based on the measurement in (a). (c) The dependence of redshift parameter depending on T: Circles and crosses are data from numerical simulation and measurement.

4. Conclusion

In conclusion, we have designed an air helicoid waveguide and utilized the interference of two coherent beams to simulate the redshift of a Gaussian wave packet in the expanding universe. The theoretical investigation of optical interference in the helicoid waveguide shows a combined effect of diffraction and curvature on the pattern, which is neglectable in our experiment. Experimental results show that the air waveguide we designed expand the interference pattern homogeneously and the measurement is in accordance with the redshift law with high precision. It also demonstrates that the helicoid waveguide serves as an experimental realization of the parabolic gradient-index lens. Furthermore, our experimental methodology enables us to measure the wave front, providing new information for the investigation of optics in curved space. The combination of this system with other optical processes, such as nonlinear optics and quantum optics, may offer more interesting approaches to mimic phenomena in classical general relativity and quantum gravity. On the application side, our helicoid waveguide may work as a new way to control optical signals in integrated photonic devices.

Funding

National Natural Science Foundation of China (11621091, 11690033, 11704181, 61425018); National Key Research and Development Program of China (2017YFA0205700, 2017YFA0303702).

Disclosures

The authors declare no conflicts of interest.

Optics EXPRESS

References

1. E. Hubble, "A relation between distance and radial velocity among extra-galactic nebulae," Proc. Natl. Acad. Sci. U. S. A. **15**(3), 168–173 (1929).
2. N. Aghanim, Y. Akrami, M. Ashdown, J. Aumont, C. Baccigalupi, M. Ballardini, A. Banday, R. Barreiro, N. Bartolo, and S. Basak, "Planck 2018 results. VI. Cosmological parameters," arXiv preprint arXiv:1807.06209 (2018).
3. S. Alam, M. Ata, S. Bailey, F. Beutler, D. Bizyaev, J. A. Blazek, A. S. Bolton, J. R. Brownstein, A. Burden, and C.-H. Chuang, "The clustering of galaxies in the completed SDSS-III Baryon Oscillation Spectroscopic Survey: cosmological analysis of the DR12 galaxy sample," Mon. Not. R. Astron. Soc. **470**(3), 2617–2652 (2017).
4. T. Abbott, S. Allam, P. Andersen, C. Angus, J. Asorey, A. Avelino, S. Avila, B. Bassett, K. Bechtol, and G. Bernstein, "First cosmology results using type Ia supernovae from the Dark Energy Survey: constraints on cosmological parameters," Astrophys. J., Lett. **872**(2), L30 (2019).
5. L. J. Garay, J. R. Anglin, J. I. Cirac, and P. Zoller, "Sonic Analog of Gravitational Black Holes in Bose-Einstein Condensates," Phys. Rev. Lett. **85**(22), 4643–4647 (2000).
6. D. D. Solnyshkov, H. Flayac, and G. Malpuech, "Black holes and wormholes in spinor polariton condensates," Phys. Rev. B **84**(23), 233405 (2011).
7. J. Steinhauer, "Observation of self-amplifying Hawking radiation in an analogue black-hole laser," Nat. Phys. **10**(11), 864–869 (2014).
8. J. Steinhauer, "Observation of quantum Hawking radiation and its entanglement in an analogue black hole," Nat. Phys. **12**(10), 959–965 (2016).
9. S. Giovanazzi, "Hawking Radiation in Sonic Black Holes," Phys. Rev. Lett. **94**(6), 061302 (2005).
10. B. Horstmann, B. Reznik, S. Fagnocchi, and J. I. Cirac, "Hawking Radiation from an Acoustic Black Hole on an Ion Ring," Phys. Rev. Lett. **104**(25), 250403 (2010).
11. H. S. Nguyen, D. Gerace, I. Carusotto, D. Sanvitto, E. Galopin, A. Lemaître, I. Sagnes, J. Bloch, and A. Amo, "Acoustic Black Hole in a Stationary Hydrodynamic Flow of Microcavity Polaritons," Phys. Rev. Lett. **114**(3), 036402 (2015).
12. T. G. Philbin, C. Kuklewicz, S. Robertson, S. Hill, F. König, and U. Leonhardt, "Fiber-optical analog of the event horizon," Science **319**(5868), 1367–1370 (2008).
13. K. E. Webb, M. Erkintalo, Y. Xu, N. G. R. Broderick, J. M. Dudley, G. Genty, and S. G. Murdoch, "Nonlinear optics of fibre event horizons," Nat. Commun. **5**(1), 4969 (2014).
14. W. G. Unruh, "Experimental Black-Hole Evaporation?" Phys. Rev. Lett. **46**(21), 1351–1353 (1981).
15. S. Weinfurtner, E. W. Tedford, M. C. J. Penrice, W. G. Unruh, and G. A. Lawrence, "Measurement of Stimulated Hawking Emission in an Analogue System," Phys. Rev. Lett. **106**(2), 021302 (2011).
16. F. de Felice, "On the gravitational field acting as an optical medium," Gen Relat Gravit **2**(4), 347–357 (1971).
17. J. B. Pendry, D. Schurig, and D. R. Smith, "Controlling Electromagnetic Fields," Science **312**(5781), 1780–1782 (2006).
18. U. Leonhardt, "Optical Conformal Mapping," Science **312**(5781), 1777–1780 (2006).
19. H. Chen, C. T. Chan, and P. Sheng, "Transformation optics and metamaterials," Nat. Mater. **9**(5), 387–396 (2010).
20. Y. Lai, J. Ng, H. Chen, D. Han, J. Xiao, Z.-Q. Zhang, and C. T. Chan, "Illusion Optics: The Optical Transformation of an Object into Another Object," Phys. Rev. Lett. **102**(25), 253902 (2009).
21. Y. Luo, D. Y. Lei, S. A. Maier, and J. B. Pendry, "Broadband Light Harvesting Nanostructures Robust to Edge Bluntness," Phys. Rev. Lett. **108**(2), 023901 (2012).
22. H. Chen, B. Zheng, L. Shen, H. Wang, X. Zhang, N. I. Zheludev, and B. Zhang, "Ray-optics cloaking devices for large objects in incoherent natural light," Nat. Commun. **4**(1), 2652 (2013).
23. U. Leonhardt and T. G. Philbin, "General relativity in electrical engineering," New J. Phys. **8**(10), 247 (2006).
24. E. E. Narimanov and A. V. Kildishev, "Optical black hole: Broadband omnidirectional light absorber," Appl. Phys. Lett. **95**(4), 041106 (2009).
25. D. A. Genov, S. Zhang, and X. Zhang, "Mimicking celestial mechanics in metamaterials," Nat. Phys. **5**(9), 687–692 (2009).
26. Q. Cheng, T. J. Cui, W. X. Jiang, and B. G. Cai, "An omnidirectional electromagnetic absorber made of metamaterials," New J. Phys. **12**(6), 063006 (2010).
27. H. Chen, R.-X. Miao, and M. Li, "Transformation optics that mimics the system outside a Schwarzschild black hole," Opt. Express **18**(14), 15183–15188 (2010).
28. C. Sheng, H. Liu, Y. Wang, S. Zhu, and D. Genov, "Trapping light by mimicking gravitational lensing," Nat. Photonics **7**(11), 902–906 (2013).
29. A. Greenleaf, Y. Kurylev, M. Lassas, and G. Uhlmann, "Electromagnetic wormholes and virtual magnetic monopoles from metamaterials," Phys. Rev. Lett. **99**(18), 183901 (2007).
30. M. Kadic, G. Dupont, S. Enoch, and S. Guenneau, "Invisible waveguides on metal plates for plasmonic analogs of electromagnetic wormholes," Phys. Rev. A **90**(4), 043812 (2014).
31. M. Maragkou, "Electromagnetic wormholes," Nat. Photonics **8**(12), 881 (2014).
32. F. Zhong, J. Li, H. Liu, and S. Zhu, "Controlling Surface Plasmons Through Covariant Transformation of the Spin-Dependent Geometric Phase Between Curved Metamaterials," Phys. Rev. Lett. **120**(24), 243901 (2018).
33. C. Sheng, H. Liu, H. Chen, and S. Zhu, "Definite photon deflections of topological defects in metasurfaces and symmetry-breaking phase transitions with material loss," Nat. Commun. **9**(1), 4271 (2018).

Optics EXPRESS

34. E. Lustig, M.-I. Cohen, R. Bekenstein, G. Harari, M. A. Bandres, and M. Segev, "Curved-space topological phases in photonic lattices," Phys. Rev. A **96**(4), 041804 (2017).
35. A. J. Kollár, M. Fitzpatrick, and A. A. Houck, "Hyperbolic lattices in circuit quantum electrodynamics," Nature **571**(7763), 45–50 (2019).
36. V. H. Schultheiss, S. Batz, A. Szameit, F. Dreisow, S. Nolte, A. Tünnermann, S. Longhi, and U. Peschel, "Optics in curved space," Phys. Rev. Lett. **105**(14), 143901 (2010).
37. V. H. Schultheiss, S. Batz, and U. Peschel, "Hanbury Brown and Twiss measurements in curved space," Nat. Photonics **10**(2), 106–110 (2016).
38. R. Bekenstein, Y. Kabessa, Y. Sharabi, O. Tal, N. Engheta, G. Eisenstein, A. J. Agranat, and M. Segev, "Control of light by curved space in nanophotonic structures," Nat. Photonics **11**(10), 664–670 (2017).
39. J. Zhu, Y. Liu, Z. Liang, T. Chen, and J. Li, "Elastic Waves in Curved Space: Mimicking a Wormhole," Phys. Rev. Lett. **121**(23), 234301 (2018).
40. S. Batz and U. Peschel, "Linear and nonlinear optics in curved space," Phys. Rev. A **78**(4), 043821 (2008).
41. C. Barceló, S. Liberati, and M. Visser, "Analogue models for FRW cosmologies," Int. J. Mod. Phys. D **12**(09), 1641–1649 (2003).
42. S. Weinfurtner, "Analogue model for an expanding universe," Gen Relativ Gravit **37**(9), 1549–1554 (2005).
43. R. Schützhold, M. Uhlmann, L. Petersen, H. Schmitz, A. Friedenauer, and T. Schätz, "Analogue of Cosmological Particle Creation in an Ion Trap," Phys. Rev. Lett. **99**(20), 201301 (2007).
44. P. Jain, S. Weinfurtner, M. Visser, and C. W. Gardiner, "Analog model of a Friedmann-Robertson-Walker universe in Bose-Einstein condensates: Application of the classical field method," Phys. Rev. A **76**(3), 033616 (2007).
45. N. C. Menicucci, S. Jay Olson, and G. J. Milburn, "Simulating quantum effects of cosmological expansion using a static ion trap," New J. Phys. **12**(9), 095019 (2010).
46. V. Ginis, P. Tassin, B. Craps, and I. Veretennicoff, "Frequency converter implementing an optical analogue of the cosmological redshift," Opt. Express **18**(5), 5350–5355 (2010).
47. N. Westerberg, S. Cacciatori, F. Belgiorno, F. D. Piazza, and D. Faccio, "Experimental quantum cosmology in time-dependent optical media," New J. Phys. **16**(7), 075003 (2014).
48. G. D. Valle, D. Gatti, and S. Longhi, "Friedmann-Robertson-Walker transformational technique in paraxial wave optics," J. Opt. Soc. Am. B **32**(9), 1834 (2015).
49. S. Eckel, A. Kumar, T. Jacobson, I. B. Spielman, and G. K. Campbell, "A rapidly expanding Bose-Einstein condensate: an expanding universe in the lab," Phys. Rev. X **8**(2), 021021 (2018).
50. I. I. Smolyaninov and Y.-J. Hung, "Modeling of time with metamaterials," J. Opt. Soc. Am. B **28**(7), 1591–1595 (2011).
51. S. Longhi, "Quantum-optical analogies using photonic structures," Laser Photonics Rev. **3**(3), 243–261 (2009).
52. S. Weinberg, *Cosmology* (Oxford University, 2008).